

Intrinsic rotation driven by non-Maxwellian equilibria in tokamak plasmas

M. Barnes,^{1,2,*} F. I. Parra,¹ J. P. Lee,¹ E. A. Belli,³ M. F. F. Nave,⁴ and A. E. White¹

¹*Plasma Science and Fusion Center, Massachusetts Institute of Technology, Cambridge, MA 02138, USA*

²*Oak Ridge Institute for Science and Education, Oak Ridge, TN 37831, USA*

³*General Atomics, PO Box 85608, San Diego, CA 92168-5608, USA*

⁴*Associação EURATOM/IST, Instituto de Plasmas e Fusão Nuclear, Instituto Superior Técnico, Technical University of Lisbon, Portugal*

The effect of small deviations from a Maxwellian equilibrium on turbulent momentum transport in tokamak plasmas is considered. These non-Maxwellian features, arising from diamagnetic effects, introduce a strong dependence of the radial flux of co-current toroidal angular momentum on collisionality: As the plasma goes from nearly collisionless to weakly collisional, the flux reverses direction from radially inward to outward. This indicates a collisionality-dependent transition from peaked to hollow rotation profiles, consistent with experimental observations of intrinsic rotation.

Introduction. Observational evidence from magnetic confinement fusion experiments indicates that axisymmetric toroidal plasmas (tokamaks) that are initially stationary develop differential toroidal rotation even in the absence of external momentum sources [1–5]. This ‘intrinsic’ rotation can depend sensitively on plasma density and current, with relatively small variations reversing the rotation direction from co- to counter-current [3, 6–9]. Conservation of angular momentum dictates that the intrinsic rotation is determined by momentum transport within the plasma. Since turbulence is the dominant transport mechanism in fusion plasmas [10], one must understand turbulent momentum transport to understand intrinsic rotation.

For the up-down symmetric magnetic equilibria used in most experiments, the turbulent momentum transport for a non-rotating plasma can be shown to be identically zero [11–13] unless one retains formally small effects that are usually neglected in analysis. A self-consistent, first-principles theory has been formulated that includes these effects [14, 15]. Of these effects, only radial variation of plasma profile gradients [16–19] and slow variation of turbulence fluctuations along the mean magnetic field [20] have been studied, and these studies have not led to a theory that explains the key dependences of intrinsic rotation in the core of tokamaks.

In this Letter we consider the novel effect of small deviations from an equilibrium Maxwellian distribution of particle velocities on turbulent momentum transport. These deviations arise naturally due to diamagnetic effects in plasmas with curved magnetic fields and pressure gradients [21]. They vary strongly with quantities such as collisionality, plasma current, and the equilibrium density and temperature gradients in the plasma. We show using direct numerical simulations that these non-Maxwellian features, though small, introduce significant new dependences to the turbulent momentum transport. We discuss the physical origins of the dependences and possible implications for tokamak experiments.

Momentum transport model. Tokamak plasma dynamics typically consist of low amplitude, small scale

turbulent fluctuations on top of a slowly evolving macroscopic equilibrium. It is thus natural to employ a mean field theory in which the particle distribution function, f , is decomposed into equilibrium, F , and fluctuating, δf , components. The fluctuations are low frequency, ω , relative to the ion Larmor frequency, Ω , and anisotropic with respect to the equilibrium magnetic field, with characteristic scales of the system size, L , along the field and the ion Larmor radius, ρ , across the field. Expanding $f = f_0 + f_1 + \dots$, employing the smallness parameter $\rho_* \doteq \rho/L \sim \omega/\Omega \sim \delta f/F \sim f_{j+1}/f_j \ll 1$, and averaging over the fast Larmor motion and over the fluctuation space-time scales, one obtains a coupled set of multiscale gyrokinetic equations for the fluctuation and equilibrium dynamics [22–26].

Typically only the lowest order system of equations for δf is considered. However, these equations have been shown to possess a symmetry that prohibits momentum transport in a non-rotating plasma [11–13]. Consequently, we include in our analysis higher order effects arising from corrections to the lowest order (Maxwellian) equilibrium [14, 15]. We limit our analysis to these non-Maxwellian corrections because they are known to depend sensitively on plasma collisionality and current, which are key parameters controlling intrinsic rotation in experiments [3, 6–9]. We further simplify analysis by considering only electrostatic fluctuations and by performing the subsidiary expansions $\rho_* \ll \nu_* \ll 1$ and $\rho_* \ll B_\theta/B \ll 1$, where B is the magnitude of the equilibrium magnetic field, B_θ is the magnitude of the poloidal component, $\nu_* \doteq \nu_{ii}qR/v_{ti}$, ν_{ii} is the ion-ion collision frequency, $v_{ti} = \sqrt{2T_i/m_i}$ is the ion thermal speed, T_i is the equilibrium ion temperature, m_i is the ion mass, q is a measure of the pitch of the magnetic field lines called the safety factor, and R is the major radius of the torus. These are good expansion parameters in typical fusion plasmas.

Using $(\mathbf{R}, \varepsilon, \mu)$ variables, with \mathbf{R} the position of the center of a particle’s Larmor motion, $\varepsilon = mv^2/2$ the particle’s kinetic energy, $\mu = mv_\perp^2/2B$ the particle’s magnetic moment, v the particle’s speed, and \perp indicating

the component perpendicular to the magnetic field, the resulting equation for the fluctuation dynamics is

$$\begin{aligned} \frac{Dg_s}{Dt} + (\mathbf{v}_{\parallel} \cdot \nabla_{\parallel} + \mathbf{v}_{Ds} \cdot \nabla_{\perp}) \left(g_s - Z_s e \langle \varphi \rangle \frac{\partial \hat{F}_s}{\partial \varepsilon} \right) \\ = -\langle \delta \mathbf{v}_E \rangle \cdot \left(\nabla_{\perp} g_s + \nabla \hat{F}_s + \frac{m_s R v_{\parallel}}{T_s} F_{Ms} \nabla \omega_{\zeta, E} \right) \quad (1) \\ + Z_s e \mathbf{v}_{\parallel} \cdot \nabla \hat{\Phi} \frac{\partial g_s}{\partial \varepsilon} + C_s, \end{aligned}$$

where $g = \langle \delta f_1 + \delta f_2 \rangle$, \mathbf{v} is particle velocity, the subscripts \parallel and \perp denote the components along and across the equilibrium magnetic field, Ze is particle charge, $\varphi = \delta \phi_1 + \delta \phi_2$ and $\hat{\Phi} = \Phi_0 + \Phi_1$ are fluctuating and equilibrium electrostatic potentials, $\hat{F} = F_0 + F_1$, $D/Dt = \partial/\partial t + \mathbf{v}_E \cdot \nabla_{\perp}$, $\langle \cdot \rangle$ is an average over Larmor radius at fixed \mathbf{R} , \mathbf{v}_{Ds} is the drift velocity due to the Coriolis effect and due to curvature and inhomogeneity in the equilibrium magnetic field, $\delta \mathbf{v}_E = (c/B) \hat{\mathbf{b}} \times \nabla_{\perp} \varphi$ and $\mathbf{v}_E = (c/B) \hat{\mathbf{b}} \times \nabla \hat{\Phi}$ are $E \times B$ drift velocities, $\hat{\mathbf{b}}$ is the unit vector directed along the magnetic field, $\omega_{\zeta, E} = -(c/RB_{\theta})(\partial \Phi_0/\partial r)$ is the toroidal rotation frequency due to $E \times B$ flow, c is the speed of light, the subscript s denotes species, and C_s describes the effect of Coulomb collisions on species s .

Tokamak plasmas are sufficiently collisional that the distribution of particle velocities is close to Maxwellian; i.e., $f_0 = F_0 = F_M$, with F_M a Maxwellian. Equilibrium deviations from F_M are determined by the drift kinetic equation [21],

$$\mathbf{v}_{\parallel} \cdot \nabla H_{1s} + \mathbf{v}_{Ms} \cdot \nabla F_{Ms} = C_s [H_{1s}], \quad (2)$$

where $H_1 = F_1 + Ze\Phi_1 F_M/T$. Finally, the electrostatic potentials are obtained and the system closed by enforcing quasineutrality:

$$\sum_s Z_s \int d^3 \mathbf{v} \left(g_s + \frac{Z_s e}{T_s} (\langle \varphi \rangle - \varphi) F_{Ms} \right) = 0, \quad (3)$$

$$\sum_s Z_s \int d^3 \mathbf{v} \left(H_{1s} - \frac{Z_s e}{T_s} \Phi_1 F_{Ms} \right) = 0. \quad (4)$$

With g_s and φ determined by Eqs. (1)-(4), the turbulent radial fluxes of energy, Q , and toroidal angular momentum, Π , are given by

$$Q_s = \langle \varepsilon_s \delta f_s \delta \mathbf{v}_E \cdot \nabla r \rangle_{\Lambda}, \quad (5)$$

$$\Pi = \sum_s \langle m_s R^2 \delta f_s (\mathbf{v} \cdot \nabla \zeta) \delta \mathbf{v}_E \cdot \nabla r \rangle_{\Lambda}, \quad (6)$$

where $\delta f = g + Ze(\langle \varphi \rangle - \varphi)F_M/T$, ζ is toroidal angle, and $\langle a \rangle_{\Lambda} = \int dt \int d^3 \mathbf{r} \int d^3 \mathbf{v} a / \int dt \int d^3 \mathbf{r}$ is an integral over all velocity space and over a volume of width w ($\rho \ll w \ll L$) and time interval Δt ($R_0/v_{ti} \ll \Delta t \ll \rho_*^{-2} R_0/v_{ti}$) encompassing several turbulence correlation lengths and times.

TABLE I: Collisionality dependence of $\omega_{\zeta, d}$

ν_*	0.003	0.030	0.059	0.089	0.148	0.208	0.297
$\frac{R_0 \omega_{\zeta, d}}{v_{ti}}$	0.091	0.114	0.127	0.137	0.153	0.165	0.180
$\frac{R_0^2}{v_{ti}} \frac{\partial \omega_{\zeta, d}}{\partial r}$	-0.447	-0.577	-0.651	-0.701	-0.776	-0.829	-0.891

Results and analysis. We obtain the correction, F_1 , to the equilibrium Maxwellian and the corresponding electrostatic potential, Φ_1 , by solving Eqs. (2) and (4) using the drift kinetic code NEO [27]. These quantities are then input to the δf gyrokinetic code GS2 [28], which we have modified to solve Eqs. (1) and (3) in the presence of F_1 and Φ_1 . To calculate the ‘intrinsic’ momentum flux that is present even for a non-rotating plasma, we set the total toroidal angular momentum in a flux surface, which consists of diamagnetic and $E \times B$ contributions, to zero: $\sum_s \langle (m_s R^2 \mathbf{v} \cdot \nabla \zeta) f_s \rangle_{\Lambda} = \sum_s m_s n_s \langle R^2 \rangle_{\Lambda} (\omega_{\zeta, E} + \omega_{\zeta, d}) = 0$, with $\omega_{\zeta, d} = \sum_s \langle m_s R^2 (\mathbf{v} \cdot \nabla \zeta) F_{1s} \rangle_{\Lambda} / \sum_s m_s n_s \langle R^2 \rangle_{\Lambda}$ the diamagnetic contribution to the toroidal rotation frequency and n the number density. The non-zero $E \times B$ rotation needed to cancel the diamagnetic rotation breaks the symmetry of the lowest order gyrokinetic equation and thus contributes to momentum transport, as do the non-Maxwellian equilibrium corrections we have included.

We consider a simple magnetic equilibrium with concentric circular flux surfaces known as the Cyclone Base Case [29], which has been benchmarked extensively in the fusion community. The equilibrium is fully specified by the Miller model [30], with $q = 1.4$, $\hat{s} \doteq \partial \ln q / \partial \ln r = 0.8$, $\epsilon \doteq r/R_0 = 0.18$, $R_0/L_n = 2.2$, and $R_0/L_T = 6.9$, where: r is the minor radius at the constant pressure surface, or flux surface, of interest; R_0 is the major radius evaluated at $r = 0$; and L_n and L_T are the density and temperature gradient scale lengths for both ions and electrons. In order to obtain the gradient of F_1 appearing in Eq. (1), we must additionally specify the radial dependence of these quantities. For our base case, we choose R_0/L_n , R_0/L_T , and dq/dr to be constant in radius.

With these base case parameters specified, we conduct a series of simulations with kinetic electrons and deuterium ions, varying ν_* and $\kappa \doteq R_0^2 d^2 \ln T / dr^2$ about the baseline value of $\nu_* = 0.003$, $\kappa = 0$. Our GS2 simulations use 32 grid points in the coordinate parallel to the magnetic field (the poloidal angle), 12 grid points in ε , 37 grid points in $\lambda = \mu/\varepsilon$, and 128 and 22 Fourier modes in the radial and binormal coordinates, respectively. The box size in both the radial and binormal coordinates is approximately $125\rho_i$.

The resulting Π/Q_i values as a function of ν_* are shown in Fig. 1. We normalize Π by Q_i , which is always positive, to remove any dependence of overall tur-

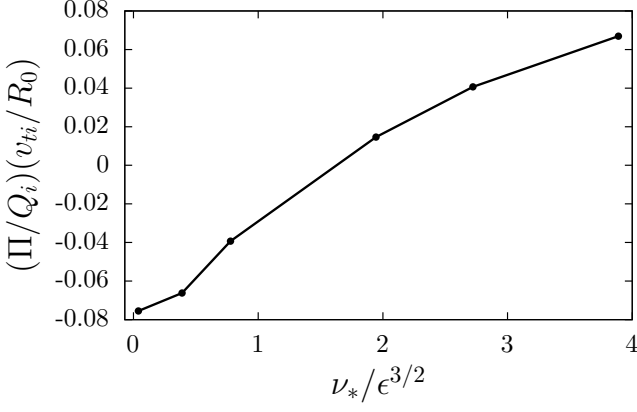


FIG. 1: Ratio of radial fluxes of ion toroidal angular momentum, Π , and energy, Q_i , vs. normalized ion-ion collision frequency, ν_* .

bulence amplitude on collisionality. Note that F_1 , and thus $\omega_{\zeta,E} = -\omega_{\zeta,d}$, varies with collisionality, as indicated in Table I. For nearly collisionless plasmas, Π/Q_i is negative, indicating a radially inward flux of co-current angular momentum that would contribute to a centrally peaked rotation profile. The ratio Π/Q_i increases with ν_* , passing through zero and becoming positive when $\nu_* \sim \epsilon^{3/2}$. For $\nu_* \gtrsim \epsilon^{3/2}$, the radially outward flux of co-current angular momentum would contribute to a hollow rotation profile.

In Fig. 2, we show results from a series of simulations in which we independently set the $E \times B$ rotation (including its derivative) and the diamagnetic effects, represented by F_1 , to zero. These are given by the blue and red curves, respectively. We see that the $E \times B$ rotation causes an inward momentum flux, with Π/Q_i increasing in magnitude with ν_* . The non-Maxwellian correction F_1 gives a Π/Q_i that goes from slightly negative to large and positive as ν_* is increased. A partial cancellation between these effects gives the actual Π/Q_i .

To explore in more detail the origin of the sign reversal of Π/Q_i , it is convenient to express the ion energy flux in the diffusive form $Q_i = -\chi_i dT_i/dr$, and to decompose the momentum flux into diffusive, advective, and other pieces:

$$\begin{aligned} \Pi = & -mR_0^2 \left(\frac{\partial \omega_{\zeta,d}}{\partial r} \chi_{\phi,d} + \frac{\partial \omega_{\zeta,E}}{\partial r} \chi_{\phi,E} \right) \\ & - mR_0 (\omega_{\zeta,d} P_d + \omega_{\zeta,E} P_E) + \Pi_{\text{other}}, \end{aligned} \quad (7)$$

where $\chi_{\phi,d}$ and P_d are diffusion and advection (commonly called ‘pinch’) coefficients, respectively, for the diamagnetic rotation, and $\chi_{\phi,E}$ and P_E play the same roles for the $E \times B$ rotation. The quantity Π_{other} accounts for all other sources of Π that arise due to $F_1(\omega_{\zeta,d}(r) = \omega_{\zeta,E}(r) = 0)$; e.g., the equilibrium parallel heat flow and other higher order velocity moments of F_1 will contribute

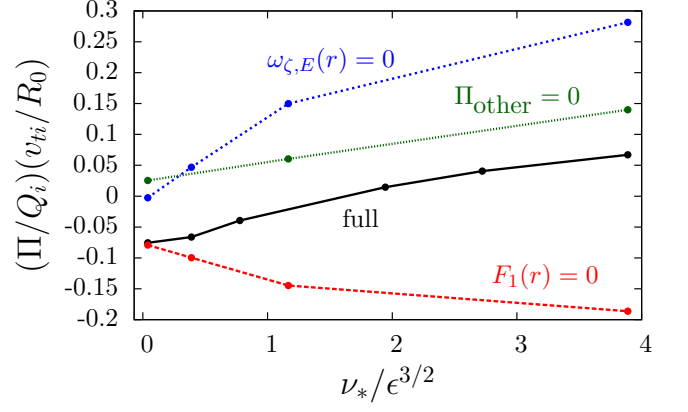


FIG. 2: Ratio of radial fluxes of ion toroidal angular momentum, Π , and energy, Q_i , vs. normalized ion-ion collision frequency, ν_* for: the base simulations (black), simulations with no $E \times B$ rotation to balance the diamagnetic rotation (blue), simulations with no correction, F_1 , to the Maxwellian equilibrium (red), and simulations with $\Pi_{\text{other}} = 0$ (green).

to Π_{other} . Using the fact that $\omega_{\zeta,E} = -\omega_{\zeta,d}$ for a non-rotating plasma, we have

$$\Pi = -mR_0 \left(R_0 \frac{\partial \omega_{\zeta,d}}{\partial r} \chi_{\phi,\text{eff}} + \omega_{\zeta,d} P_{\text{eff}} \right) + \Pi_{\text{other}}, \quad (8)$$

where $\chi_{\phi,\text{eff}} = \chi_{\phi,d} - \chi_{\phi,E}$ and $P_{\text{eff}} = P_d - P_E$.

Changing ν_* can alter Π/Q_i in multiple ways. First, the turbulent advection and diffusion coefficients, P_{eff}/χ_i and $\chi_{\phi,\text{eff}}/\chi_i$, can be modified either directly by collisions or indirectly by the ν_* -dependent rotation and rotation gradient. By independently varying ν_* , $\omega_{\zeta,E}$, and $\partial \omega_{\zeta,E}/\partial r$ in GS2 turbulence simulations with fixed F_1 and Φ_1 , we found that such modifications of the advection and diffusion coefficients were minor. Furthermore, the turbulence type, characterized by the dominant linear instability mechanism, remained the same (ion-temperature-gradient driven) for all simulations.

With $\chi_{\phi,\text{eff}}/\chi_i$ and P_{eff}/χ_i approximately independent of ν_* , we see from Eq. (8) that the ν_* dependence of $(\Pi - \Pi_{\text{other}})/Q_i$ comes entirely from the change of $\omega_{\zeta,d}$ and $\partial \omega_{\zeta,d}/\partial r$ with ν_* , given in Table I. In order to calculate $(\Pi - \Pi_{\text{other}})/Q_i$, we ran a series of simulations in which we used a modified F_1 that was constrained to produce pure rotation so that $\Pi_{\text{other}} = 0$. The results are shown as the green curve in Fig. 2. We see that $(\Pi - \Pi_{\text{other}})/Q_i$ is always positive and increases approximately linearly with $\partial \omega_{\zeta,d}/\partial r$, as diffusion was found to dominate over advection in these cases. This indicates that equal and opposite diamagnetic and $E \times B$ rotations do not lead to a complete cancellation of momentum transport [31]. The increase in $(\Pi - \Pi_{\text{other}})/Q_i$ with ν_* accounts for just over half of the total increase in Π/Q_i over the range of ν_* we have considered. The rest of the increase, as well as the negative offset needed to give the sign reversal in Π/Q_i must come from Π_{other}/Q_i .

TABLE II: Temperature profile dependence of $\omega_{\zeta,d}$

$-L_T^2 \frac{\partial^2 \ln T}{\partial r^2}$	-1	0	1	2	4
$\frac{R_0^2}{v_{ti}} \frac{\partial \omega_{\zeta,d}}{\partial r}$	-1.116	-0.447	-0.105	0.223	0.835

To see how these results may be modified for different plasma profiles, we also conducted a series of simulations in which we fixed $\nu_* = 0.003$ and varied $\kappa = R_0^2 \partial^2 \ln T / \partial r^2$. Since the calculation of F_1 in NEO depends on R_0/L_T , varying κ affects $\partial F_1 / \partial r$ but not F_1 itself. Consequently, $\partial \omega_{\zeta,d} / \partial r$ varies with κ (see Table II) while $\omega_{\zeta,d}$ itself remains fixed. The change in Π/Q_i with κ is shown in Fig. 3. As was the case in the ν_* study, the $E \times B$ and F_1 contributions to Π/Q_i partially cancel, though in this case each contribution independently changes sign with κ . The net result is a relatively weak variation of Π/Q_i with no sign reversal.

Discussion. The sign reversal of Π/Q_i shown in Fig. 1 suggests a transition from peaked to hollow rotation profiles when $\nu_* \sim \epsilon^{3/2}$. This is consistent with experimental results, which show such transitions at similar ν_* values when density (proportional to ν_*) is increased or current (inversely proportional to ν_*) is decreased [3, 6, 9, 32]. Furthermore, our observation that the normalized turbulence diffusion and advection coefficients vary only minimally during the transition agree with recent experimental observations showing that the fundamental turbulence characteristics are unaltered as the rotation reverses direction [9].

From Fig. 2 and the analysis following Eq. (8), it is evident that a combination of effects leads to the sign reversal of Π/Q_i . However, the sign reversal fundamentally originates from the ν_* dependence of F_1 , which has been extensively studied and is the main concern of ‘neoclassical’ theory (see, e.g., [21, 33]). For $\nu_* \ll \epsilon^{3/2}$, known as the ‘banana’ regime, all particle orbits are collisionless. However, for $\epsilon^{3/2} \ll \nu_* \ll 1$, known as the ‘plateau’ regime, low energy particles that are trapped in the equilibrium magnetic well become collisional. For a plasma perfectly in the banana or plateau regimes, one can show that F_1 , and thus our Π/Q_i , becomes independent of ν_* [21, 33]. It is only when transitioning between these regimes that Π/Q_i varies with ν_* . So, while different profiles of quantities such as density, temperature, and current may alter or eliminate the transitions with ν_* discussed above, they can only occur for $\nu_* \sim \epsilon^{3/2}$.

Finally, we reiterate that in our analysis we retained small terms (namely the diamagnetic effects that give rise to departures from a Maxwellian equilibrium distribution) in the multiscale gyrokinetic expansion, while we neglected other terms (radial profile variation, certain effects arising from the slow variation of fluctuations along the magnetic field, etc.) that may be of the same size.

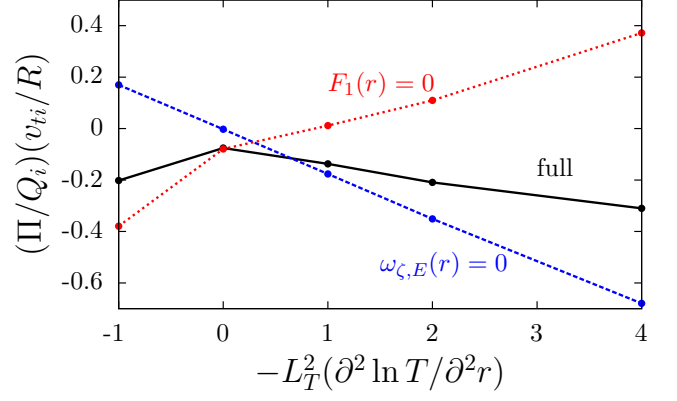


FIG. 3: Ratio of radial fluxes of ion toroidal angular momentum, Π_i , and energy, Q_i , vs. normalized second derivative of the logarithmic ion temperature for: the base simulations (black) and for simulations with no $E \times B$ flow to balance the diamagnetic flow (red) and no correction, F_1 , to the Maxwellian equilibrium (blue).

There are two justifications for this. First, if the fluctuation amplitudes and scales do not vary strongly with B_θ/B , then the diamagnetic effects considered here dominate so that our model is fully self-consistent [14, 15]. Second, the small effects we have neglected are not expected to have a particularly strong dependence on collisionality. Thus, while inclusion of these effects may provide an offset to the momentum transport, we do not expect them to modify the variation of Π/Q_i with ν_* presented here.

We thank J. Candy and P. J. Catto for useful discussions. M.B. was supported by a US DoE FES Postdoctoral Fellowship, F.I.P. was supported by US DoE Grant No DE-FG02-91ER-54109, and computing time was provided by the National Energy Scientific Computing Center, supported by the Office of Science of the U.S. Department of Energy under Contract No. DE-AC02-05CH11231.

* Electronic address: mabarnes@mit.edu

- [1] J.-M. Noterdaeme *et al.*, Nucl. Fusion **43**, 274 (2003).
- [2] J. S. deGrassie *et al.*, Phys. Plasmas **11**, 4323 (2004).
- [3] A. Bortolon, B. P. Duval, A. Pochelon, and A. Scarabosio, Phys. Rev. Lett. **97**, 235003 (2006).
- [4] J. E. Rice *et al.*, Nucl. Fusion **47**, 1618 (2007).
- [5] F. I. Parra *et al.*, Phys. Rev. Lett. **108**, 095001 (2012).
- [6] B. P. Duval *et al.*, Plasma Phys. Control. Fusion **49**, B195 (2007).
- [7] A. Ince-Cushman *et al.*, Phys. Rev. Lett. **102**, 035002 (2009).
- [8] L.-G. Eriksson *et al.*, Plasma Phys. Control. Fusion **51**, 044008 (2009).
- [9] A. E. White *et al.*, Phys. Plasmas, accepted.

- [10] G. D. Conway, Plasma Phys. Control. Fusion **50**, 124026 (2008).
- [11] A. G. Peeters and C. Angioni, Phys. Plasmas **12**, 072515 (2005).
- [12] F. I. Parra, M. Barnes, and A. G. Peeters, Phys. Plasmas **18**, 062501 (2011), arXiv:1102.3717.
- [13] H. Sugama, T. H. Watanabe, M. Nunami, and S. Nishimura, Plasma Phys. Control. Fusion **53**, 024004 (2011).
- [14] F. I. Parra, P. J. Catto, and M. Barnes, Nucl. Fusion **51**, 113001 (2011), arXiv:1102.4613.
- [15] F. I. Parra, M. Barnes, I. Calvo, and P. J. Catto, Phys. Plasmas **19**, 056116 (2012), arXiv:1203.4958.
- [16] P. H. Diamond *et al.*, Phys. Plasmas **15**, 012303 (2008).
- [17] W. X. Wang *et al.*, Phys. Plasmas **17**, 072511 (2010).
- [18] R. E. Waltz, G. M. Staebler, and W. M. Solomon, Phys. Plasmas **18**, 042504 (2011).
- [19] Y. Camenen, Y. Idomura, S. Jolliet, and A. G. Peeters, Nucl. Fusion **51**, 073039 (2011).
- [20] T. Sung *et al.*, (2013), arXiv:1302.6453.
- [21] F. L. Hinton and R. D. Hazeltine, Rev. Mod. Phys. **25**, 239 (1976).
- [22] H. Sugama and W. Horton, Phys. Plasmas **4**, 405 (1997).
- [23] M. Barnes, Ph.D. thesis, University of Maryland, 2008, arXiv:0901.2868.
- [24] M. Barnes *et al.*, Phys. Plasmas **17**, 056109 (2010), arXiv:0912.1974.
- [25] F. I. Parra and P. J. Catto, Plasma Phys. Control. Fusion **52**, 045004 (2010).
- [26] I. G. Abel *et al.*, Reports on Progress in Physics, submitted (2012).
- [27] E. A. Belli and J. Candy, Plasma Phys. Control. Fusion **50**, 095010 (2008).
- [28] W. Dorland, F. Jenko, M. Kotschenreuther, and B. N. Rogers, Phys. Rev. Lett **85**, 5579 (2000).
- [29] A. M. Dimits *et al.*, Phys. Plasmas **7**, 969 (2000).
- [30] R. L. Miller *et al.*, Phys. Plasmas **5**, 973 (1998).
- [31] J. P. Lee, F. I. Parra, and M. Barnes, Phys. Rev. Lett., submitted (2013), arXiv:1301.460.
- [32] J. E. Rice *et al.*, Nucl. Fusion **51**, 083005 (2011).
- [33] P. Helander and D. J. Sigmar, Collisional transport in magnetized plasmas (Cambridge University Press, Cambridge, 2002).